Shear Capacity of Rectangular Duct Panel Experiencing Internal Pressure

K. S. Sivakumaran, T. Thanga, B. Halabieh

Abstract—The end panels of a large rectangular industrial duct, which experience significant internal pressures, also experience considerable transverse shear due to transfer of gravity loads to the supports. The current design practice of such thin plate panels for shear load is based on methods used for the design of plate girder webs. The structural arrangements, the loadings and the resulting behavior associated with the industrial duct end panels are, however, significantly different from those of the web of a plate girder. The large aspect ratio of the end panels gives rise to multiple bands of tension fields, whereas the plate girder web design is based on one tension field. In addition to shear, the industrial end panels are subjected to internal pressure which in turn produces significant membrane action. This paper reports a study which was undertaken to review the current industrial analysis and design methods and to propose a comprehensive method of designing industrial duct end panels for shear resistance.

In this investigation, a nonlinear finite element model was developed to simulate the behavior of industrial duct end panel, along with the associated edge stiffeners, subjected to transverse shear and internal pressures. The model considered the geometric imperfections and constitutive relations for steels. Six scale independent dimensionless parameters that govern the behavior of such end panel were identified and were then used in a parametric study. It was concluded that the plate slenderness dominates the shear strength of stockier end panels, and whereas, both the plate slenderness and the aspect ratio influence the shear strength of slender end panels. Based on these studies, this paper proposes design aids for estimating the shear strength of rectangular duct end panels.

Keywords—Thin plate, transverse shear, tension field, finite element analysis, parametric study, design.

I. INTRODUCTION

HEAVY industrial processes often require transport of large amount of high pressure air/gases through series of steel ducts. The positive or negative gas pressure inside the ducts may be in the range of 10 to 15 kPa. The cross-sectional dimensions of such industrial rectangular ducts may be in the range of 5 m to 15 m and thus, in some ways they are quite unique structures. In such duct work, which is essentially a box girder type bridge, the vertical loads such as self-weight, weight of insulation, dust load, etc., are transferred to the side walls as shear (which act as web) and then to the end supports. Thus, the plate panels of the sidewalls adjacent to the support legs are subjected to large shear loads, as well as internal

K. S. Sivakumaran is a Professor, Department of Civil Engineering, McMaster University, Hamilton, Ontario, Canada, L8S 4L7 (e-mail: siva@mcmaster.ca).

T. Thanga is a Senior Structural Engineer, Hatch Ltd, Mississauga, Ontario, Canada, L5K 2R7.

B. Halabieh is the President, and an Engineer, BAH Enterprises Inc, Oakville, Ontario, Canada, L6H 1Z6.

pressure. This paper is concerned with the shear capacity of end panels of industrial rectangular ducts, which are subjected to concurrent transverse shear and internal pressures.
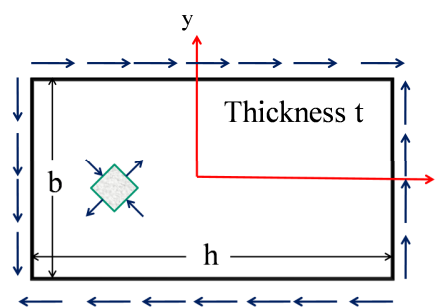
II. BEHAVIOR OF THIN PLATES UNDER SHEAR

Fig. 1 Thin plate subjected to shear

Consider a thin rectangular steel panel having a width b, length h and thickness t, subjected to shear stress τ along all four edges. Such a panel experiences in-plane tensile and compressive stresses σ acting at 45° to the shear axis, as shown in the stress element. This diagonal compressive stresses σ, whose magnitude is equal to the applied shear stress τ, can cause buckling of the plate when the applied shear stress τ reaches the shear buckling stress τ_{cr} given as $\tau_{cr} = k_v \pi^2 E/[12(1-v^2)(b/t)^2]$, where, E is the elastic modulus , v is the Poisson`s ratio and k_v is the shear buckling coefficient. For simply supported plates $k_v = 5.35 + 4.0\ (b/h)^2$ and for clamped plates $k_v = 8.98 + 5.6\ (b/h)^2$. In the above expressions, b is the width of shorter dimension of the long plate [1]. The buckling stress τ_{cr} increases with decreasing plate slenderness (b/t), and the stocky plates may yield in shear at $\tau_y = F_y/\sqrt{3} \approx 0.60\ F_y$ prior to buckling, where F_y is the tensile yield strength of steel. The demarcation plate slenderness (b/t) for the shear yielding/buckling can be obtained by equating τ_y to shear buckling stress τ_{cr}. The resulting (b/t) for a simply supported steel plate with the aspect ratio (b/h)= 1 (using elastic modulus $E = 200,000$ MPa and yield strength of $F_y = 350$ MPa) will be about 90. The actual (b/t) associated with the side wall plate of a large industrial duct, which is defined, as the ratio of the stiffener spacing to the plate thickness, will be in the range of 125 to 350. Thus, in such plates the applied shear stress will cause elastic buckling, however, the plate panel has the capacity to carry additional shear load beyond buckling because of the stable tensile stresses those may be generated in the diagonal directions. This is referred to as tension-field action or post-buckling strength. Based on extensive studies on the post

World Academy of Science, Engineering and Technology
International Journal of Civil and Environmental Engineering
Vol:9, No:12, 2015

buckling behavior of the web panels by Basler [2], the AISC [3] first included the post buckling strength in its specification. Interest in the mechanics and post-buckling capacity of panels subjected to shear continues to exist as reflected by some of the recent studies [4]-[7]. The ultimate shear strength for the slender web panel in the current AISC specification [8] is given by; $V_u = 0.6F_y ht[C_v + (1 - C_v)])/1.15\sqrt{1 + (b/h)^2}$, where $C_v = (\tau_{cr}/0.6F_y)$. The first term in the above equation represents the contribution of the buckling shear resistance. The second term in the bracket is the post-buckling shear strength due to one band of uniform diagonal tension field across the web. The aspect ratio (h/b) of end panels of industrial rectangular ducts, however, may be higher than 2, thus, potentially, such panels can develop several bands of tension fields across the length of the plate when subjected to uniform shear. Furthermore, the end panel between stiffeners is subjected to lateral pressure load due to gases, which produces bending stresses σ_b and the diaphragm stresses σ_m perpendicular to the stiffener direction, which are not accounted for in the above Vu expression [8]. This study investigates the impact of these two factors on the shear strength (including post-buckling strength) of industrial duct end panels. Here, a finite element method based parametric study was conducted to investigate these issues.

III. THE FINITE ELEMENT ANALYSIS MODEL FOR INDUSTRIAL DUCT END PANELS

The buckling behavior of plate panels, including the post-buckling behavior, can be conveniently investigated using the finite element analysis method. This method can easily establish the deformations and stresses of a plate panel subjected to shear loads and pressure loads. It can be used to obtain their collapse loads and the associated modes as well. A schematic of duct side panel selected for the investigation and the parametric study presented in this paper is shown Fig. 2.
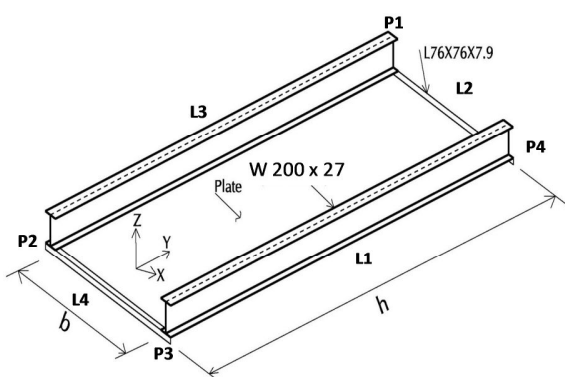
Fig. 2 Schematic of an end panel

The duct side panel consists of a plate panel bounded by two adjacent stiffeners and the corner angles at its top and bottom edges. Angles of designation L76X76X7.9mm (dimensions of the legs in mm. and thickness of the angle in mm) and stiffener of designation W200x27 (depth of a wide flange section in mm and weight per meter in kg), which are

somewhat of a representative sizes, were selected for this study. The finite element model for the problem was developed using a commercial general purpose nonlinear finite element program ADINA [9], which has an extensive element library, material models and modeling capabilities appropriate for a nonlinear problem, such as the one under consideration. Fig. 3 shows the finite element model of the problem, details of which are discussed below.
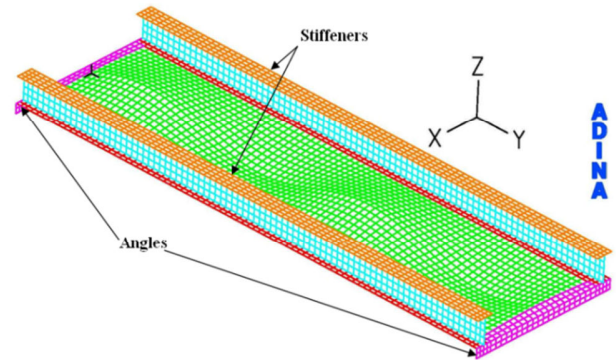
Fig. 3 The finite element model

A 4-node shall element, based on updated Lagrangian formulation, from ADINA element library was used to model the entire plate panel. This element can be used to model both thick and thin shell problems that require the Mindlin plate theory, and for large displacement and small strain problems. The available maximum of seven integration points through thickness were used for this analysis in order to capture the stress variation across the thickness, and thus to ensure accurate initiation and development of tension fields across the plate. To simulate shear loading, uniformly distributed line loads were applied along all four-plate edges. Increasing loads were applied until collapse of the structure. A displacement controlled analysis strategy, utilizing the arc-length iterative scheme, was utilized in order achieve equilibrium convergence of the nonlinear load-displacement path.

A. Initial Geometric Imperfections

Inevitably, geometric imperfections, such as out-of-flatness of the plate, camber, or sweep of structural members, exist in structural elements. The magnitude and shape of initial geometric imperfection play a significant role in the response and the ultimate strength of end panels. As can be seen in Fig. 3, an imperfection pattern consisting of a half sine wave in transverse direction and a series of half sine waves in the longitudinal direction was introduced in the finite element model. Thus, the initial geometric imperfection distribution is $\Delta_{imp} = \Delta_o \sin(\pi x/b)(\pi y/b)$, where, Δ_o in the peak amplitude of the initial imperfection, and b is the width of the plate panel. As shown in Fig. 2, the x coordinate is in the transverse direction of the plate panel and the y coordinate is in the longitudinal direction of the plate panel, whereas h is the dimension of the plate in the y direction, which is the height of the plate panel. The permissible out-of-flatness of a steel plate corresponding to fabrication related initial imperfections

World Academy of Science, Engineering and Technology
International Journal of Civil and Environmental Engineering
Vol:9, No:12, 2015

was given in [10] as $\Delta o/t = 0.025 \left[(b/t)\sqrt{Fy/E} \right]^2$. In the analysis large industrial duct, such as the one under consideration, the deflected shape of the plate panel subjected to transverse pressure load should also be incorporated since such plate panels are subjected to in-plane shear forces as well as transverse pressure load. The deflected shape of the long plate panel due to transverse pressure can be assumed to be cylindrical type. The relation between the plate slenderness and the normalized deflection (Δ_p/t), due to lateral pressure corresponding to first yield (i.e. yielding of the outer fiber) was established in [11]. Thus, the finite element mesh shown in Fig. 3, contains a pattern of initial geometric imperfection which was the summation of the cylindrical deformation due to lateral pressure and the double sine function representing the out-of-flatness of the plate panel.

B. Material Model

The plate, stiffener sections, and corner angles were assumed to be made of ASTM A36 mild-carbon steel for this study. An idealized elastic-plastic-strain hardening tri-linear material model was used to model the material constitutive behavior of the ASTM A36 steel. The salient points of this model are; modulus of elasticity E= 200000MPa, the yield strength $F_y = 250$MPa, and the nominal strain at yield is thus $\varepsilon_y = Fy/E = 0.00125$. The strain at initiation of strain hardening was taken as $10\varepsilon_y$. A linear relationship is presumed in the strain hardening range, with a strain hardening modulus E_{st} for mild carbon steels taken as E/30. The tensile strength F_u, for A36 steel is 400MPa. The material models in ADINA [9] are based on incremental theories in which the total strain increment is decomposed into an elastic strain increment and a plastic strain increment. An incremental plasticity model is formulated in terms of yield surface, flow rule and a hardening rule. The von Mises yield surface is used to specify the state of stresses corresponding to start of plastic flow. The von Mises yield surface assumes that yielding metal has the form of a cylinder in three dimensional principal stress space. The von Mises criterion also uses the associated flow rule for the development of plastics stress-strain relations of metals. The associated flow is the plastic flow developed along the direction normal to yield surfaces. A hardening rule specifies the yield surface during plastic flow. In this study, the isotropic hardening rule was selected. In the isotropic hardening rule, the size of the yield surface changes uniformly in all directions as plastic straining occurs. The isotropic hardening rule is ideal for a static nonlinear analysis of this plate panel subjected to shear.

C. Boundary Conditions

As shown in Fig. 2, the origin of the coordinate system is at the mid-height of the plate, $x - y$ plane coincides with the middle plane of the plate panel, and the z-axis is perpendicular to the plate. Consider u_1, u_2, and u_3 as the translations along the x, y, and z directions, respectively and θ_1, θ_2, and θ_3 as the rotations about the x, y, and z directions, respectively. The edges of the plate panel are labeled L_1, L_2, L_3 and L_4 the four corners of the plate panel are marked as P_1, P_2, P_3 and P_4. The

translation in z direction was restrained along the all edges. The translation along x direction was restrained at the corner point P_1 while the translation along x and y directions were restrained at the point P_2 to avoid any rigid body rotation. The industrial ducts are often simply supported at their ends using support rings. Furthermore, the ducts are allowed to freely expand and contract along their longitudinal axis through a provision of sliding support rings. Therefore, the x - translations of the longer edges were not restrained, and it was assumed that the whole longer edges will be experience the same amount of x-translation due to continuity of plate panels. In order to simulate this uniform translation of longer edges, the translation along the x direction were constrained to be the same along the edges L_1 and L_3. The rotational stiffness of the longer edges of the plate panel (h dimension) depends on the rotational stiffness provided by the stiffeners connected to those edges, which will be in-between a fixed edge and a simply supported edge. As shown in Fig. 2, in this study the W200X27 stiffener was completely modeled using plate elements. In order to provide the rotational stiffness along the plate and flange juncture, the rotation about the y direction were restrained along the edges L_1 and L_3. The flange edges of the stiffeners, however, were not restrained against the rotation along the y- direction.

D. Mesh Density and Validation Study

A convergent study was performed in order to establish a suitable mesh density for this numerical study. A square plate having dimensions b= $1000mm$, $h = 1000mm$ and $t = 5mm$ was subjected to increasing uniform shear load. The amplitude of the double sine function for out-of-flatness of the plate is 6.25mm. The investigation considered five identical plate models with different mesh densities. The density of the coarse mesh is 6x6, while the density of the finer mesh is 26x26. The percentage changes in ultimate strength of each model having different mesh densities were established and compared. The percentage change in ultimate strength for increasing mesh density of 6x6, 10x10, 16x16, 20x20 and 26x26 were 7.4%, 3.0%, 2.2% and 1.1%, respectively. It was determined that a reasonable degree of accuracy can be attained with a coarser mesh density, however, a very dense mesh of shell elements is desirable in order to trace the nonlinear equilibrium path into the unloading regime due to the severity of the material and geometric nonlinearities associated with the plate panel subjected to shear. Thus, a mesh density of 16x16 was selected. In Physical dimensions, each element size is approximately 62.5 mm x 62.5 mm. In order to validate the model, the model developed for the convergence study was first applied to a square plate subjected to uniform shear, for which theoretical buckling results (211 kN) exist. The applied shear versus the out of plane deflection at the middle of the plate was extracted for each loading step (time step). In general, it is difficult to distinguish between the pre- buckling and post-buckling responses of an imperfect plate subjected to uniform shear, since no bifurcation point exists for such plates. However various techniques exist which can be used to obtain buckling load from numerical

World Academy of Science, Engineering and Technology
International Journal of Civil and Environmental Engineering
Vol:9, No:12, 2015

experimental results. Using one of those techniques, here, two tangent lines were drawn from two points having the largest rate of slope change and the intersection of the two tangents was taken as the buckling load. The buckling load so obtained was around 210kN which was in close agreement to the theoretical results.
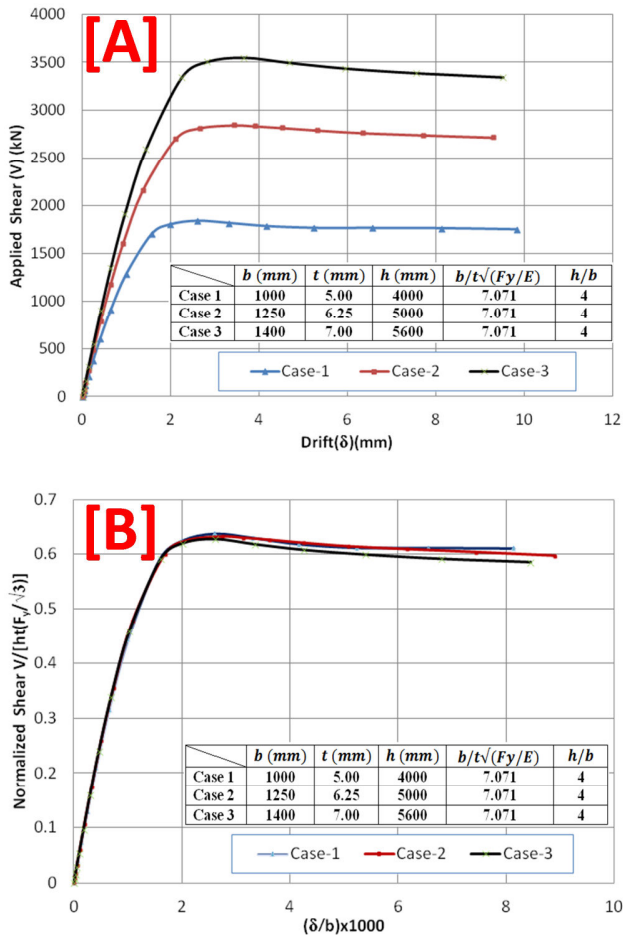
IV. PARAMETRIC STUDY

Fig. 4 Applied shear versus drift relation and Normalized shear and normalized drift relations

First let us identify the dimensionless parameters those control the behavior and the ultimate strength of the industrial duct end panel. These dimensionless parameters must be independent of any scale and material characteristic. The fundamental parameters governing the plate panel are the geometric parameters of plate such as width of the side panel b, height of the side plate panel h, thickness of the plate t, and the response parameters such as initial out-of-plane deflection Δ and the diaphragm stress σ_m. It should be noted here the Δ is the algebraic sum of magnitude of initial geometric imperfection Δ_o and the deflection Δp due to the internal pressure. The material parameters of influence are the modulus of elasticity E (or elastic shear modulus G) and the yield strength of the plate material F_y. The loading parameter is the applied shear V and the output variable is selected as the

in-plane drift δ. Using Buckingham Pi-theorem [12] the above identified nine fundamental parameters can be reduced to six dimensionless parameters that govern the behavior, including the ultimate strength, of end panel plates. They are (1) the plate slenderness $b/t\sqrt{(Fy/E)}$, (2) the aspect ratio h/b, (3) the normalized shear $V/[ht(Fy/\sqrt{3})]$, (4) the normalized drift δ/b, (5) the normalized initial deflection Δ/t, and (6) the normalized diaphragm stress σ_m/Fy. A previous study [11], that considered a strip of plate subjected lateral pressure load, established a relation between $b/t\sqrt{(Fy/E)}$, and the dimensionless load parameter $pE/(Fy)^2$. That study [11] also established the corresponding deflections of the plate $\Delta p/t$, and the diaphragm stress σ_m/Fy. Therefore, for a particular value of plate slenderness $b/t\sqrt{(Fy/E)}$, the associated total initial out-of-plane deflections Δ/t and σ_m/Fy are the known quantities. Thus, for the problem under consideration, the parameters $b/t\sqrt{(Fy/E)}$, and h/b are the plate dimensional parameters, normalized shear $V/[ht(Fy/\sqrt{3})]$ is the loading parameter and δ/b is the output parameter. Three different end plate panels were considered in order to verify the completeness and the scale independence of the dimensionless parameters identified above. The three plate panels had the same dimensionless parameters $b/t\sqrt{(Fy/E)}$, and h/b but with different scale. The actual dimensions of these plates are given in the insert of Fig. 4. The corresponding dimensionless parameters Δ/t, and σ_m/Fy were incorporated for this analysis even though these would be constant for the plate panels with the same slenderness parameter $b/t\sqrt{(Fy/E)}$.

Fig. 4 (A) shows the applied shear versus the drift for the three plate cases considered. These plots are different as the scale of fundamental parameters, the shear and the drift are not dimensionless. However, the normalized applied shear versus normalized drift plots shown on Fig. 4 (B) is identical. Therefore, it can be concluded that the change of scale does not affect the non-dimensional representation of the response, provided the analysis models have the same dimensionless parameters.

In this investigation, a detailed parametric study was conducted to establish the ultimate shear capacity of the industrial duct side plate panels having different dimensions. The material properties were not varied and the modulus of elasticity $E = 200000 MPa$ and yield strength of $F_y = 250 MPa$ were used for this parametric study. The plate slenderness b/t for the side plate panels considered ranged from 125 to 350 in steps of 25. The corresponding dimensionless parameters $b/t\sqrt{F_y/E}$ (and the associated dimensionless parameters $\Delta p/t$ and σ_m/F_y corresponding to first yield due to internal pressure) were 4.419 (0.86,0.88), 5.303 (1.13,0.1), 6.187 (1.38,0.117), 7.7071 (1.65,0.127), 7.955 (1.91,0.136), 8.839 (2.17,0.141), 9.723 (2.42,0.146), 10.607 (2.67,0.151), 11.490 (2.91,0.154) and 12.374 (3.15,0.158). A review of the aspect ratio h/b of the practical duct configurations revealed that its range is approximately from 2 to 10. Each of the plates satisfying the above parametric values was analyzed until collapse, from which the shear load V versus in plate drift δ history and the

World Academy of Science, Engineering and Technology
International Journal of Civil and Environmental Engineering
Vol:9, No:12, 2015

corresponding ultimate load were obtained. For each analysis model, the load versus drift history was converted into the dimensionless form, thus, into normalized shear $V/[ht(Fy/\sqrt{3})]$ versus normalized drift δ/b history. A representative deformed shape of the side plate panel with $b/t\sqrt{F_y/E} = 7.071$ and $h/b = 5$, at the peak shear load, is shown in Fig. 5
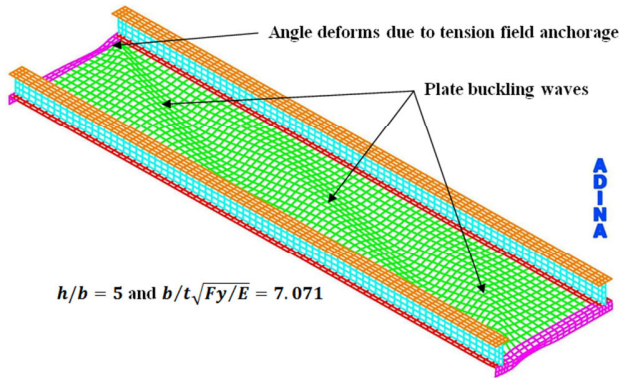

Fig. 5 Deformed shape of end panel at ultimate load levels

Fig. 6 shows the normalized shear versus normalized drift history plots for side plate panels having a fixed $b/t\sqrt{F_y/E} = 7.955$ and varying aspect ratios h/b. For each panel aspect ratio, the slope of the linear portion of the responses represents a non-dimensional stiffness. The initial non-dimensional stiffness associated with these plates was the same. However, as the aspect ratio increases, the predicted normalized ultimate shear strength decreases slightly. It was also observed that increasing aspect ratio h/b from 2 to 10 results in increasing number of tension field's bands. In general, the orientation of these tension fields within the stiffeners are the same, except at the top and bottom tension fields which tend to propagate

towards the intersection of the angle and the stiffener. Ideally, the boundary members should have enough flexural stiffness in order to adequately anchor the tension fields. Inadequate flexural stiffness afforded by the angles at top and bottom of side panel prevents adequate anchoring of the tension fields resulting in angles experiencing local deformations, as shown in Fig. 5. From the normalized shear versus normalized drift history plots the normalized ultimate shear capacity $Vu/[ht(Fy/\sqrt{3})]$ of all the plates under consideration were extracted. In order to understand the influence of various parameters on the ultimate normalized shear strengths of duct side panels, the variation of $Vu/[ht(Fy/\sqrt{3})]$ with respect to $b/t\sqrt{F_y/E}$ and h/b were plotted in a three-dimensional representation. The Fig. 7 shows the resulting plot.
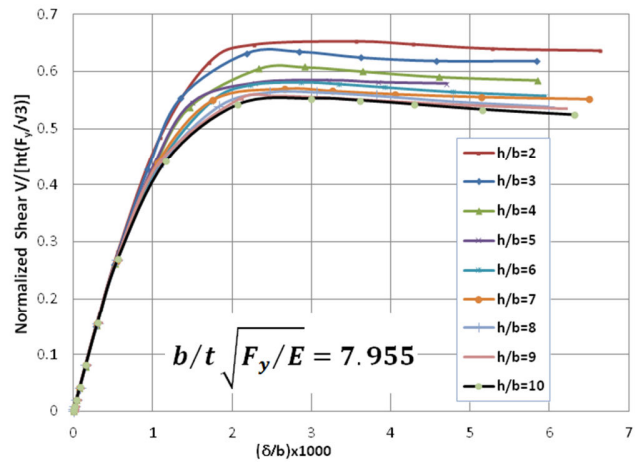

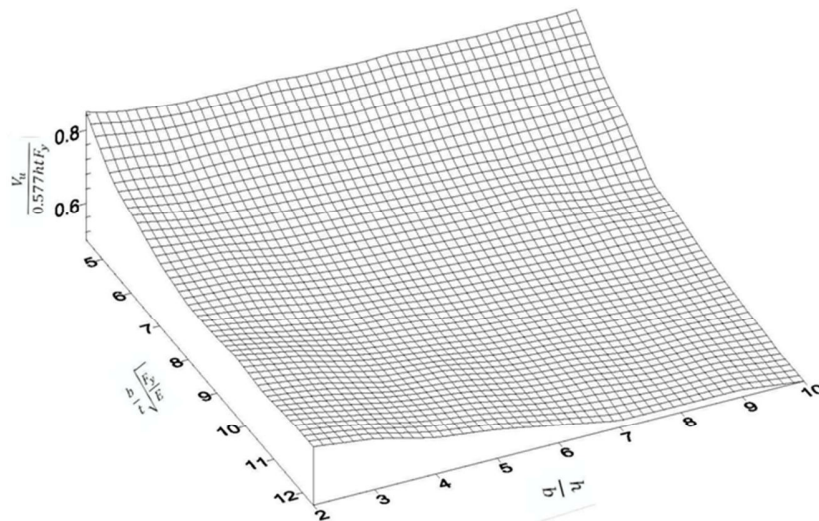Fig. 6 Impact of h/b on the normalized shear versus drift relations

Fig. 7 Three-dimensional representation of the shear capacity of industrial duct side panels

From Fig. 7, it can be observed that the plate slenderness $b/t\sqrt{F_y/E}$ significantly influences the normalized ultimate shear strength, particularly when its value is less than about 6.

In this range, the aspect ratios h/b seem to have a minimal effect. However, for side plate panels with plate slenderness more than 6 (i.e. slender plates), the ultimate shear strength

depends on both, the plate slenderness $b/t\sqrt{F_y/E}$ and the aspect ratio h/b. Although the three-dimensional graphs provide the general pattern how the normalized shear strength is influenced by dimensionless parameters, contour plots of $Vu/[ht(Fy/\sqrt{3})]$ with respect to parameters $b/t\sqrt{F_y/E}$ and h/b might be more practical for design engineers. Such plots were established as part of this investigation; however, they are not given in the paper. These are some of the observations associated with those contour plots. The shear strength of stockier plates, represented by $b/t\sqrt{F_y/E} < 6,$ does not depend on the plate aspect ratio, and that those plates can carry more than 65% of shear yield strength concurrently with the internal pressures. On the other hand, the aspect ratio seems to influence the normalized ultimate shear strength of slender plates, defined here as $b/t\sqrt{F_y/E} > 6.$ Fig. 7 shows normalized ultimate shear strengths up to a value of 50% of shear yield strength $Vu/[ht(Fy/\sqrt{3})] \approx 0.5$. The stockier side plate panels show gradual loss in normalized shear capacity with the increase in the plate slenderness $b/t\sqrt{F_y/E}$ for a particular aspect ratio h/b.

V. Concluding Remarks

The ultimate shear resistance V_u of the slender side plate panels of large rectangular industrial ducts consists of plate shear buckling strength and the post-buckling strength due to tension field action. However, hitherto, the impact of internal pressure on the shear strength had not been investigated. Furthermore, higher aspect ratio of such plate panels may result in several bands of tension fields, which may provide additional contribution to the post-buckling strength. A finite element model of a duct side panel consisting of a plate panel bounded by two adjacent stiffeners and the corner angles at its top and bottom was built and verified. The model included initial geometrical imperfection, and realistic material models associated with structural steels. The out-of-plane deflections and the diaphragm stresses due to internal pressures, established in a previous study [11], was incorporated into the analysis model to account the effects of lateral pressures on the shear capacity of end panels. In this study, firstly, the dimensionless parameters affecting the behavior of the side panel subjected to shear were identified and relevant non-dimensional parameters were derived. A parametric study was conducted considering the practical range of these dimensionless parameters. For designers convenience, the contours of normalized ultimate shear strengths were established, which indicate that the shear capacity of stockier end panels $b/t\sqrt{F_y/E} < 6,$ depend on the slenderness rather than the aspect ratio, and the associated capacity is more than 65% of the corresponding shear yield resistance. The aspect ratio influences the ultimate shear strength of slender end panels of a rectangular industrial duct.

References

[1] Timoshenko, S. P., Gere, J. M., (1961), "Theory of Elastic Stability." 2nd Edition. McGraw-Hill, New York.

[2] Basler, K. (1961), "Strength of Plate Girders in Shear." Journal of the Structural Division, In Proceedings of the American Society of Civil Engineers 87 (ST7), 151-180.

[3] AISC ASD, (1963), "Manual of Steel Construction- Allowable Stress Design" American Institute of Steel Construction, Chicago.

[4] Porter, D.M. Rockey, K.C. and Evans, H.R. (1975), The collapse behavior of plate girders loaded in shear, Structural Engineer, Vol. 53, No.8, , pp. 313–325.

[5] Marsh C, Ajam W, and Ha H. (1988), Finite element analysis of postbuckled shear webs. Journal of Structural Engineering, Vol. 114, No. 7, pp.1571–87.

[6] Yoo, C.H., and Lee, S.C. (2006), Mechanics of web panel postbuckling behavior in shear, Journal of Structural Engineering, Vol. 132, No. 10, pp.1580–9.

[7] Alinia, M. M. Maryam, Shakiba, and Habashi, H.R. (2009), Shear failure characteristics of steel plate girders, Thin-Walled Structures, Vol. 47, No. 12, pp.1498–506.

[8] AISC, (2010) Specification for Structural Steel Buildings, ANSI/AISC 360-10, American Institute of Steel Construction, Chicago, Illinois, U.S.A.

[9] ADINA, (2009), ADINA 8.5 user manual, ADINA R & D Inc, Watertown, MA, USA.

[10] Paik, J. K., and Thayamballi, A.K., (2003), "Ultimate Limit State Design of Steel-Plated Structures" Wiley, Edition 1.

[11] Thanga, T., Sivakumaran, K. S., and Halabieh, B., (2013), "Stiffened Plates of Rectangular Industrial Ducts", Canadian Journal of Civil Engineering, Vol. 40, No. 4: pp. 334-342 (April, 2013).

[12] Langhaar, H.L., (1951), "Dimensional Analysis and Theory of Models." John Wiley, N.Y.